Regulation of Physiological Rates in *Caenorhabditis elegans* by a tRNA-Modifying Enzyme in the Mitochondria

Jason Lemieux, Bernard Lakowski,[1] Ashley Webb, Yan Meng, Antonio Ubach, Frédéric Bussière, Thomas Barnes[2] and Siegfried Hekimi

Department of Biology, McGill University, Montréal, Québec H3A 1B1, Canada

Manuscript received January 25, 2001
Accepted for publication June 11, 2001

ABSTRACT

We show that the phenotype associated with *gro-1(e2400)* comprises the whole suite of features that characterize the phenotype of the *clk* mutants in *Caenorhabditis elegans*, including deregulated developmental, behavioral, and reproductive rates, as well as increased life span and a maternal effect. We cloned *gro-1* and found that it encodes a highly conserved cellular enzyme, isopentenylpyrophosphate:tRNA transferase (IPT), which modifies a subset of tRNAs. In yeast, two forms of the enzyme are produced by alternative translation initiation, one of which is mitochondrial. In the *gro-1* transcript there are also two possible initiator ATGs, between which there is a sequence predicted to encode a mitochondrial localization signal. A functional GRO-1::GFP fusion protein is localized diffusely throughout the cytoplasm and nucleus. A GRO-1::GFP initiated from the first methionine is localized exclusively to the mitochondria and rescues the mutant phenotype. In contrast, a protein initiated from the second methionine is localized diffusely throughout the cell and does not rescue the mutant phenotype. As oxygen consumption and ATP concentration have been reported to be unaffected in *gro-1* mutants, our observations suggest that GRO-1 acts in mitochondria and regulates global physiology by unknown mechanisms.

THE *clk* class of genes of the nematode *Caenorhabditis elegans* affects the timing of cellular, developmental, and behavioral features of the worm (Hekimi *et al.* 1995; Wong *et al.* 1995; Lakowski and Hekimi 1996; Branicky *et al.* 2000). Affected features include the cell cycle, embryonic and postembryonic development, rhythmic adult behaviors, reproductive rates, and life span. The period, duration, or rate of these processes appears to be deregulated, resulting in an average slowing down (Wong *et al.* 1995). *clk* gene mutants can be phenotypically rescued by a maternal effect, a phenomenon that has been most extensively documented for *clk-1* (Wong *et al.* 1995). That is, homozygous mutants derived from heterozygous mothers are phenotypically wild type except for the rate of egg production. This means that most phenotypes can be observed only in the second homozygous generation. In fact, all three *clk* genes were identified in a screen designed to identify viable maternal-effect mutations (Hekimi *et al.* 1995). However, given that adult animals are >500 times larger than the egg, it is surprising that maternal rescue is possible for physiological features of the adult. This observation, together with other data on *clk-1* (Wong *et al.* 1995; Branicky *et al.* 2000), has been interpreted to suggest that the *clk* genes can induce an epigenetic state during early development that is maintained throughout the life of the animal.

One aspect of the phenotype of *clk* mutants that has attracted particular attention is their increased life span (Lakowski and Hekimi 1996). Both the average and maximum life spans of *clk-1*, *-2*, and *-3* mutants exceed those of the wild type. In addition, these mutations can also act synergistically, such that double mutants live substantially longer than the component single mutants (Lakowski and Hekimi 1996). Moreover, double mutants of *clk-1* with *daf-2*, another gene that has been implicated in life span regulation in *C. elegans* (Kenyon *et al.* 1993), also live a very long time, from three to five times longer than the wild type (Lakowski and Hekimi 1996). We have argued that these observations, as well as other data, suggest that *clk* mutants live long because they live slowly (Hekimi *et al.* 1998; Hekimi 2000). It should be noted, however, that the metabolic rates of *clk* mutants are not reduced in any simple fashion (Braeckman *et al.* 1999; Felkai *et al.* 1999; Miyadera *et al.* 2001), and it remains unclear, therefore, which progeric process has been attenuated in *clk* mutants.

clk-1 was cloned and found to encode a mitochondrial protein (Felkai *et al.* 1999) that is structurally and functionally highly conserved throughout the eukaryotes (Ewbank *et al.* 1997) and in those prokaryotes whose genome is most similar to that of mitochondria (Hekimi 2000). *clk-1* mutants do not make ubiquinone (coen-

Corresponding author: Siegfried Hekimi, Department of Biology, McGill University, 1205 Ave. Dr. Penfield, Montréal, Québec H3A 1B1, Canada. E-mail: siegfried.hekimi@mcgill.ca

[1] *Present address:* Genzentrum, Ludwig-Maximilians Universität Feodor-Lynen-Str. 25, D-81377 Munich, Germany.

[2] *Present address:* Millenium Pharmaceuticals, 640 Memorial Dr. 3W, Cambridge, MA 02139.

zyme Q), a crucial lipid cofactor in the respiratory chain (Jonassen *et al.* 2001; Miyadera *et al.* 2001), but respire by using demethoxyubiquinone instead (Miyadera *et al.* 2001). In an attempt to reconcile a number of disparate observations, including the mitochondrial localization of CLK-1, the maternal effect, the absence of severe metabolic phenotypes, and the general deregulation of physiological rates observed in *clk* mutants, we proposed a model in which *clk-1* affects, directly or indirectly, the mechanisms by which the state of mitochondrial function is relayed to the nucleus to modulate gene expression (Felkai *et al.* 1999; Branicky *et al.* 2000). Such cross talk between the mitochondria and the nucleus has been observed in several systems (Biswas *et al.* 1999; Frolov *et al.* 2000; Sekito *et al.* 2000; Amuthan *et al.* 2001) and likely serves to adapt the pattern of nuclear gene expression to changes in the metabolic state of the organism.

To test our hypothesis further, we are characterizing genetically and molecularly other *clk-1*-like genes. One such gene is *gro-1*, which was originally isolated as a slow-growing mutant segregating from a wild-type strain (PaC1) distinct from the standard *C. elegans* wild-type strain N2 (Hodgkin and Doniach 1997). Partial early characterization of the *gro-1* mutants also indicated that, like the *clk* gene mutants, they had an increased life span (Lakowski and Hekimi 1996). Furthermore, as for *clk-1*, the overall metabolic capacity of *gro-1* mutants was found to be essentially unaffected (Braeckman *et al.* 1999).

Here we present further genetic characterization of *gro-1*, its molecular identification, subcellular pattern of expression, and the subcellular localization required for its function. We also briefly discuss how the molecular identity of GRO-1, which is the highly conserved cellular enzyme isopentenylpyrophosphate:tRNA transferase, and its requirement in the mitochondria lends credence to a role for *clk* genes in mitochondrial/nuclear cross talk.

MATERIALS AND METHODS

Genetic mapping of *gro-1*: Multipoint mapping placed *gro-1* on chromosome III, close to, but to the left of, *dpy-17* (Hodgkin and Doniach 1997), and close to the cloned gene *clk-1* (Wong *et al.* 1995; Ewbank *et al.* 1997). Although *clk-1(e2519)* and *gro-1(e2400)* map very close to each other and have very similar phenotypes, *e2400* complements *e2519*, indicating that these mutations are in different genes (Wong *et al.* 1995). By picking Lon non-Dpy recombinant progeny from *dpy-17 clk-1 lon-1/gro-1* animals, we had confirmed that *gro-1* maps very close to *clk-1* but were unable to separate *clk-1* and *gro-1* (Hekimi *et al.* 1995). We now mapped *gro-1* 0.03 cM to the left of *clk-1*. For this, the following experiments were performed: *gro-1/dpy-17 unc-32* [*dpy-17* **4** *gro-1* **51** *unc-32*]; *dpy-17gro-1/++* [0/220 Dpys developed quickly, $p < 0.2$ cM]; *gro-1lon-1/++* [2/250 Lons developed quickly, $p = 0.4$ cM]; *dpy-17gro-1sma-4/unc-79clk-1lon-1* [84 Dpy non-Sma recombinants: *dpy-17* **15** *gro-1* **69** *sma-4*]; *dpy-17gro-1sma-4/unc-79clk-1lon-1* [*unc-79* **44** *dpy-17* **5** *gro-1* **0** *clk-1* **4** *lon-1*]; *dpy-17gro-1sma-4/unc-79clk-1lon-1* [Sma non-Dpy recombinants: *dpy-17* **22** *gro-1* **3** *clk-1* **27** *lon-1* **27** *sma-4*]; *sDp3* includes *gro-1(e2400)*; *sDf121* deletes *gro-1(e2400)*.

Moving *gro-1* from the PaC1 to the N2 background: To remove linked PaC1 sequences from *gro-1(e2400)*, the *gro-1(e2400)* mutation was first flanked on the left and on the right by the two closest morphological markers, *dpy-17(e164)* and *lon-1(e185)*, respectively. The *dpy-17(e164) gro-1(e2400) lon-1(e185)* triple mutant was then outcrossed three times to remove unlinked sequences. These markers were then removed in several steps. First, the closest marker, *dpy-17(e164)*, was removed by crossing *unc-79(e1030)* males into the *dpy-17(e164) gro-1(e2400) lon-1(e185)* strain and picking Lon non-Dpy recombinants. In this way, a *unc-79(e1030) gro-1(e2400) lon-1(e185)* strain was generated. This strain was then outcrossed with N2 males and Unc non-Lon recombinants were picked to generate a *unc-79(e1030) gro-1(e2400)* strain. Finally, this *unc-79(e1030)gro-1(e2400)* strain was outcrossed an additional time with N2 males and 340 non-Unc F2 progeny were placed individually on plates. Four of the 340 F_3 broods developed slowly and segregated ¼ Uncs [putative *unc-79(e1030) gro-1 (e2400)/ gro-1(e2400)* strains]. From one of these plates non-Unc progeny were picked individually to new plates to generate a homozygous *gro-1(e2400)* strain, which was given the strain name MQ520. In this process, unlinked chromosomes were outcrossed nine times, presumably removing almost all unlinked PaC1 sequences.

PCR amplification: For PCR reactions using clean abundant template, a single pair of primers was used. The notation A:B is used here, where A is the first primer and B the second. In cases where the template of interest is rare and nonspecific amplification is likely, nested PCR was used. The notation A/C:D/B is used here, where A and B are the primers in the first reaction and C and D are the primers in the second "nested" reaction. The sequences of all primers cited can be obtained from S.H. upon request.

Construction of clones for rescuing experiments: The deletion construct pMQ2 was made by deleting a 29.9-kb SpeI fragment of ZC395. The frameshift construct pMQ4 was made by cutting pMQ2 at a unique *Apa*I site in the second predicted exon of ZC395.7 and degrading the resulting 4-bp overhang with mung bean nuclease. pMQ5 was made by cutting pMQ2 at a unique *Nde*I site in the second predicted exon of ZC395.6 and filling in the resulting 2-bp overhang with the Klenow fragment of DNA polymerase. pMQ8 is a construct in which residues 27,230–27,522 of cosmid C34E10 were fused to residues 1524–3678 of cosmid ZC395. The region of C34E10 is the region immediately 5′ of the *gop-1* coding sequence and encodes the entire intragenic region between *gop-1* and C34E10.8, which is a transcript in the opposite direction. It must thus contain the entire promoter of the *gro-1* operon. The region from ZC395 contains the entire *gro-1* coding sequence as well as 23 nucleotides 5′ of the initiator ATG and 134 nucleotide 3′ of the stop codon. To construct this clone we performed recombinant PCR, using hybrid primers, that is, single primers complementary to more than one DNA fragment. The hybrid primers, which were complementary in part to the promoter sequence and in part to the *gro-1* coding sequence, were SHP159 and SHP160. The flanking primers used were SHP161 and SHP162, which had the restriction site for *Sac*I and *Pst*I, respectively, built into their 5′ ends. Three sequential PCR reactions were performed. The first PCR reaction used the primers SHP161 and SHP160 and N2 genomic DNA as template to amplify the promoter. The second PCR reaction used the primers SHP159 and SHP162 and N2 genomic template to amplify *gro-1*. The third PCR reaction used the flanking primers SHP161 and SHP162 and the gel-purified products from the first and the second PCR reaction as tem-

plate to fuse the two products. The high-fidelity polymerase VENT (New England Biolabs, Beverly, MA) was used.

Construction of clones for expression experiments: The *gro-1::gfp* clone pMQ418 was constructed using vector pPD95.77 (a generous gift from A. Fire). The construct pMQ8 (see above) was used as template for amplification with SHP151:SHP170. SHP151 and SHP170 contain overhangs that will incorporate *Sph*I and *Xba*I restriction sites into the PCR product, respectively, to allow for the ligation of the fragment (containing the *gro-1* promoter and coding sequence) into the *Sph*I/*Xba*I sites of pPD95.77.

Clone pMQ418 was used as template for site-directed mutagenesis [Stratagene (La Jolla, CA) site-directed mutagenesis kit] to construct clones pMQ420 (using primers SHP1860: SHP1861) in which the first potential initiator ATG is changed to ATC, pMQ421 (using primers SHP1862:SHP1863) in which the second potential initiator is changed to ATC, and pMQ419 (using primers SHP1858:SHP1859) in which the A at nucleotide position 33 between the two ATGs is removed. This creates a frameshift such that the GRO-1 protein cannot be produced after initiation from the first ATG. The sequence of all clones produced by PCR was verified by sequencing.

Identifying the *e2400* mutation: Genomic DNA was prepared by standard techniques and the primers SHP93:SHP92 (on the basis of the known genomic sequence) were used to amplify the *gro-1* region from N2, PaC1, and *gro-1(e2400)* (CB4512). The PCR regimen was 94° for 20 sec, 55° for 1 min, and 72° for 2 min, for 30 cycles. These products were sequenced with the following primers: SHP93, -94, -95, -96, -97, -98, -99, -100, and -92.

Establishing splicing and *trans*-splicing patterns: RNA was extracted by standard methods from mixed-stage worms and used to make reverse-transcribed cDNA libraries (Frohman *et al.* 1988). To determine which of the genes upstream of *gro-1* were transcribed in the same operon, the 5′ end of each was amplified using SL1 or SL2 primers. The SL1/2 primers were used in conjunction with a gene-specific primer. A second round of PCR, using the same SL primer but a different internal primer, was then performed to obtain a very specific product. For *gop-1* the internal primer pair used was SHP141/SHP142 and the expected product size was ~570 bp. The primer pair for *gop-2* was SHP143/SHP144 to produce a product of ~510 bp. The primer pair SHP145/SHP146 was used to amplify the 440-bp *gop-3* 5′ end. For *ham-1*, the primer pair SHP130/SHP119 was used in the amplification of the 465-bp 5′ end. Finally, to amplify *gro-1*'s 390-bp 5′ end, the primer pair SHP95/SHP99 was used.

The primer Rt, used to amplify the cDNA library, has two primer landing pads Ri and Ro built into its 5′ end. Each of the five genes of the operon was amplified from this cDNA in a number of pieces: the 5′ end, using a primer corresponding to the *trans*-spliced leader sequence SL2 (when the gene was *trans*-spliced; see below) and two internal primers, and the 3′ end using the primers Ri and Ro along with an internal primer. This allowed priming for PCR at the end of each cDNA. *gop-1* was amplified in three parts: the 5′ part was amplified with the nested primers SHP190:SHP174/SHP176, the middle part with SHP172/SHP173:SHP176, and the 3′ end with SHP175:Ri/Ro. *gop-2* was amplified with the primers SL2:SHP143/SHP144 and SHP180:Ri/Ro. *gop-3* was amplified with the primers SL2:SHP184/SHP135 and SHP138:Ri/Ro. *hap-1* was amplified with the primers SL2:SHP99/SHP100, SHP94:SHP99/SHP100, and SHP97:Ri/Ro.

In all experiments designed to establish splicing patterns, the PCR regimen used was 94° for 20 sec, 60° for 1 min, 72° for 2 min for 30 cycles for the first PCR; and 94° for 20 sec, 60° for 1 min, 72° for 2 min for 30 cycles for the second nested PCR.

hGRO-1 sequence: The human protein sequence shown in the alignment of Figure 3 was obtained by compiling information from several sources. We sequenced a publicly available clone (c-2ec05), obtained from Genome Systems, whose partial sequence (accession nos. F07677 and Z40724) encoded a protein similar to GRO-1. We then identified overlapping clones in the database and assembled a predicted mRNA sequence for a human *gro-1* gene. Sequences that were used include the following accession nos.: AA332152, AA121465, AA847885, and NP_060116.

RESULTS

Genetic mapping of *gro-1* and transfer into the N2 genetic background: Multipoint mapping placed *gro-1* on chromosome III, close to, but to the left of, *dpy-17* (Hodgkin and Doniach 1997) and close to the cloned gene *clk-1* (Wong *et al.* 1995; Ewbank *et al.* 1997). Detailed mapping of the region allowed us to genetically separate *gro-1* from *clk-1* and map it 0.03 cM to the left of *clk-1* (see materials and methods).

Originally, the growth and life span of mutants carrying the *gro-1(e2400)* mutation were characterized in the strain CB4512 (Lakowski and Hekimi 1996; Hodgkin and Doniach 1997). This strain is derived from PaC1, a wild-type background that is phenotypically and molecularly distinct from N2, the standard background for mutations in *C. elegans* (Hodgkin and Doniach 1997). To facilitate phenotypic comparisons between *gro-1* and other genes that have been isolated in the N2 background, we transferred the *gro-1(e2400)* mutation into a background as close as possible to that of N2. To remove linked PaC1 sequences from *gro-1(e2400)*, the mutation was first flanked on the left and on the right by the two closest morphological markers, *dpy-17(e164)* and *lon-1(e185)*, respectively. These markers were then removed in several steps (see materials and methods). In this process, unlinked chromosomes were outcrossed nine times, removing almost all unlinked PaC1 sequences, while remaining linked PaC1 sequences should represent <200 kb centered around *gro-1*.

Phenotype of *gro-1* mutants: *gro-1* mutants display a general slowing down of physiological features. The affected features we scored include the duration of embryogenesis and postembryonic development, the rates of adult behaviors, and brood size (Table 1). In addition, the animals appear in general to behave sluggishly, yet they appear anatomically normal and are capable of complex behaviors such as mating for males. The most striking aspect of the phenotype, however, is the existence of a maternal effect that extends to adult phenotypes and includes development, adult behavior, and reproductive phenotypes (Table 1). In fact, homozygous *gro-1* mutants derived from a heterozygous mother are essentially indistinguishable from the wild type. On the other hand, heterozygotes produced by mating of wild-type males to homozygous *gro-1* mothers are mostly wild type except for the duration of embryonic development, which is clearly slower than that of wild-type or mater-

TABLE 1

The phenotype of *gro-1(e2400)* mutants can be rescued by a maternal effect

Phenotype[a]	Wild type (N2)	*e2400/e2400* (MQ520)	*e2400/+* from *e2400/e2400* mothers (zygotic rescue[b])	*e2400/e2400* from *e2400/+* mothers (maternal rescue[b])	+/+ and +/*e2400* from +/*e2400* mothers
Embryogenesis (hr)	13.9 ± 1.6 (n = 26)	22.5 ± 2.0 (n = 115)	17.0 ± 1.43 (n = 64)	13.7 ± 0.5 (n = 27)	13.6 ± 0.5 (n = 82)
Brood size (eggs)	302 ± 31 (n = 20)	177 ± 52) (n = 12)	248 ± 75 (n = 10)	291 ± 50 (n = 27)	291 ± 34 (n = 56)
Postembryonic development (hr)	46.8 ± 1.4 (n = 200)	104.9 ± 10.1 (n = 70)	43.2 ± 2.4 (n = 49)	47.7 ± 2.1 (n = 129)	47.5 ± 2.2 (n = 389)
Defecation cycle (sec)	54.3 ± 2.5 (n = 18)	88.6 ± 7.5 (n = 25)	52.1 ± 1.9 (n = 10)	57.8 ± 2.8 (n = 28)	54.9 ± 3.1 (n = 72)

[a] All phenotypes were scored at 20° as in Wong *et al.* (1995).

[b] Progeny from heterozygous (+/*e2400*) hermaphrodites or putative cross-progeny were placed singly on individual plates and their phenotype was scored. Their genotype was later established from the phenotype of their clonal progeny, either slow growing (*e2400/e2400*) or wild-type growth rate (+/+ or +*e2400*).

Figure 1.—*gro-1(e2400)* shows a strict maternal effect on embryonic development. The duration of embryogenesis of *gro-1*/+ animals produced by mating wild-type males to homozygous *gro-1* hermaphrodites is delayed with respect to the wild type. Embryos at the two-cell stage were dissected from gravid mothers and observed every hour until hatching as described in Wong *et al.* (1995).

nally rescued worms (Table 1 and Figure 1). This suggests that although most features can be rescued either maternally or zygotically, for embryonic development there is a strict requirement for maternal *gro-1*. In contrast, the mutant phenotype is fully expressed when the homozygous mutants are produced from a cross between heterozygous males and homozygous hermaphrodites, indicating that there is no paternal rescue (data not shown).

gro-1 mutants show an increased life span but the effect is relatively weak in the N2 genetic background (Table 2). This is in contrast to earlier findings (Lakowski and Hekimi 1996), where the effect of *gro-1* on life span was reported to be more dramatic but was scored in the PaC1 background and compared to N2 worms. To explore the effect of *gro-1* on life span more directly, we compared life spans of N2, PaC1 (CB4507), *gro-1* in the N2 background (MQ520), and *gro-1* in the PaC1 background (CB4512). We found that PaC1 animals live somewhat longer than N2 animals and that *gro-1* has a much stronger effect on life span in the PaC1 background than in the N2 background (Table 2). This suggests that some other genetic difference or differences between PaC1 and N2 are capable of synergizing with *gro-1* to increase life span. Strong synergistic effects on life span between relatively weak mutations have been observed previously (Lakowski and Hekimi 1996).

Molecular identification of *gro-1*: Genetic mapping of *gro-1* placed the gene immediately to the left of *clk-1*, a molecularly characterized gene. The relationship between the genetic and physical distances in this region of the genome (Lakowski and Hekimi 1996) indicated that *gro-1* should lie no more than 15–20 kb to the left of *clk-1*. A number of overlapping cosmids spanning this

TABLE 2

The effect of *gro-1(e2400)* on life span in different wild-type backgrounds

Strain	Life span (days) ± SEM[a] [maximum life span (days)] (*n*)[b]
N2 (wild type)	20.03 ± 0.3[a]
	SD[c] ± 4.02
	[37][d]
	(150)[b]
PaC1 (wild type)	23.1 ± 0.3[a]
	[32][d]
	(200)[b]
MQ520 [*gro-1(e2400)* in N2 background]	22.3 ± 0.5[a]
	SD[c] ± 6.45
	[43][d]
	(146)[b]
CB4512 [*gro-1(e2400)* in PaC1 background]	31.3 ± 0.9[a]
	[56][d]
	(100)[b]

[a] The error of the mean of two independently conducted experiments is given.

[b] The sample size corresponds to the total number of animals examined.

[c] To test further the significance of the difference in means of N2 and MQ520, the populations from the two independent experiments were pooled (SD, standard deviation for the pooled population), a *t*-test was performed, and a highly significant difference was found ($P < 0.001$).

[d] Maximum life span (days).

region were used for transformation rescue. Cosmids ZC395 (that contains also *clk-1*) and C34E10 were capable of fully rescuing the Gro-1 phenotype, including the slow growth and behaviors. The narrow overlap between the cosmids defined a rescuing region of ~7 kb. An ~3.5-kb deletion clone (pMQ2) of ZC395 containing the left-most end of the cosmid also produced full rescue. pMQ2 contains two predicted genes, ZC395.6 and ZC395.7. To identify which corresponds to *gro-1*, each predicted gene was tested independently for rescuing activity by introducing frame-shift mutations in the other gene (see MATERIALS AND METHODS). The clone (pMQ4) that contains an intact ZC395.6 gene but an inactivated ZC395.7 could fully rescue the phenotype, but the clone (pMQ5) that contains an intact ZC395.7 but inactivated ZC395.6 could not.

ZC395.6 was resequenced from the mutant and by comparison to the N2 sequence the *e2400* lesion was identified as a small rearrangement starting at nucleotide 2720 of ZC395 (the sequence TGCAATGTA is replaced by GC). This results in a frameshift producing a 33-amino-acid extension after the lesion in the predicted mutant protein. The lesion was not found in the *gro-1(+)* gene in the PaC1 background.

***gro-1* lies in an operon with four other genes:** Examination of genes predicted by Genefinder (http://www.sanger.ac.uk/Projects/C_elegans/webace_front_end.shtml) in the genomic sequence upstream of *gro-1* suggested that *gro-1* could lie in an operon of up to five genes. For genes to be organized into such a transcriptional unit they must share the same 5′–3′ orientation and be closely positioned (ZORIO *et al.* 1994). Approximately 70% of *C. elegans* genes are *trans*-spliced at their 5′ end to a 22-bp sequence known as *s*pliced *l*eader (SL)1. Genes downstream in operons are unique in that they are *trans*-spliced to a distinct leader (SL2; HUANG and HIRSH 1989). Therefore, the presence of SL2 in an mRNA can be used as a marker indicating a gene's membership in an operon. We examined the *trans*-splicing of four genes upstream of *gro-1*, using SL1- or SL2-specific primers in conjunction with pairs of gene-specific primers to amplify the 5′ ends of these genes from a reverse transcription (RT)-PCR-generated cDNA library (see MATERIALS AND METHODS). *gro-1* and the three genes upstream of it were all found to be spliced to SL2 (Figure 2). Therefore, *gro-1* appears to be the fifth member of a five-gene operon. We renamed the first three genes in the operon *gop-1* to *-3* (for *gro-1 op*eron). The fourth gene was named *hap-1* as it is strongly homologous to the yeast gene *ham1,* which is involved in *h*ydroxyl*a*mino*p*urine sensitivity (NOSKOV *et al.* 1996).

We also established the splicing pattern of all five genes by sequencing their cDNAs amplified from an RT-PCR library (see MATERIALS AND METHODS). In general, the predictions made by Genefinder were correct with three exceptions. What was predicted to be the last exon of *gop-3* actually splices over C34E10.9 (a small predicted gene on the complementary strand) to pick up two additional exons (Figure 2). We also found an additional intron in the predicted second exon of *gro-1*. Finally, the true *gro-1*-initiating AUG was actually 42 bp upstream of the predicted start. The sequences of all five genes are deposited in GenBank.

The molecular identity of GRO-1: The protein encoded by *gro-1* is highly similar to a highly conserved cellular enzyme, isopentenylpyrophosphate:tRNA transferase (IPT; BARTZ *et al.* 1970; CAILLET and DROOGMANS 1988; TOLERICO *et al.* 1999; STANFORD *et al.* 2000). Figure 3 illustrates the sequence conservation from *Escherichia coli* (MiaAp) to *Saccharomyces cerevisiae* (Mod5p) and *Homo sapiens* (hGRO1). The human sequence was obtained by sequencing a publicly available clone and database searches. The residue at which the *e2400* mutation truncates the protein is indicated by an asterisk in the figure. IPT catalyzes the transfer of an isopentenyl moiety to the adenosine immediately adjacent 3′ to the anticodon of tRNAs whose anticodons terminate in U. In bacteria, the gene that encodes IPT is generally called *miaA* and mutations in this gene have been studied extensively for their effect on growth and gene expression (ERICSON and BJORK 1986; BJORK *et al.* 1999). In yeast, IPT is encoded by the gene *mod5* (DIHANICH *et al.* 1987), whose products are being studied mostly for

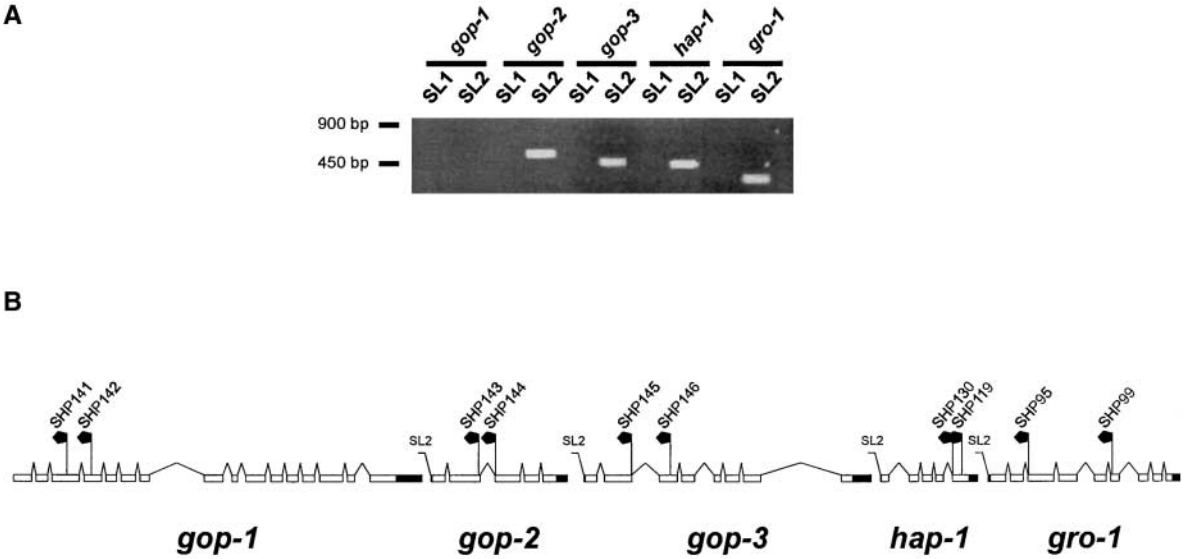

FIGURE 2.—*gro-1* is the most downstream gene in an operon containing five genes. (A) The 5′ region of the five genes forming the putative *gro-1* operon were PCR amplified from a cDNA library (see MATERIALS AND METHODS). SL1/2 primers were used with gene-specific reverse primers. No PCR bands could be detected using a SL1 forward primer for any of the five genes. However, a specific band could be detected using a SL2 forward primer for *gop-2*, *gop-3*, *hap-1*, and *gro-1*, indicating that these genes are arranged in an operon. (B) The structure of the *gro-1* operon and the intron/exon structure of all genes. The 3′ untranslated region of each gene is denoted by black boxes. The positions of gene-specific reverse primers used in A are denoted by arrows.

the mechanisms involved in their complex subcellular localization (TOLERICO *et al.* 1999). MiaAp/Mod5p-like proteins are encoded by all sequenced bacterial and eukaryotic genomes so far but appear to be absent from archaeal genomes (STANFORD *et al.* 2000). The prokaryotic and eukaryotic sequences are highly similar (Figure 3), and there appears to be only one *gro-1*-like sequence in the genome of any organism whose genome has been fully sequenced (STANFORD *et al.* 2000). The eukaryotic sequences differ mostly by a C-terminal extension that contains a predicted zinc finger motif in the human and worm sequences (Figure 3). The sequences that allow nuclear localization in *S. cerevisiae* also map to this region (TOLERICO *et al.* 1999). The other recognizable structural motif found in all IPT sequences is an ATP/GTP binding site motif (Figure 3).

Of the genes in the operon, *gop-1* to *-3* encode proteins that have highly conserved vertebrate homologs of unknown function. Only *gop-2* encodes a protein with a recognizable motif, an ATP/GTP binding site motif of the same type as GRO-1 (p-loop). The fourth gene in the operon, *hap-1*, is similar to the yeast gene HAM1, mutations in which can confer resistance to mutagenesis by 6-*N*-hydroxylaminopurine (NOSKOV *et al.* 1996) by an unkown mechanism. However, recent work on a putative homolog in the Archaea *Methanococcus jannaschii* suggests that it might be an NTPase that can hydrolyze nonstandard nucleotides (HWANG *et al.* 1999).

Expression of GRO-1: To study the expression of *gro-1* we first constructed a synthetic gene in which the *gro-1* coding sequence is placed directly adjacent to, and thus under the control of, the putative promoter sequence of the operon, that is, the intergenic sequence between *gop-1* and the next 5′ gene (C34E10.8; see MATERIALS AND METHODS). This construct (pMQ8) rescues the *gro-1* phenotype to wild-type (growth rate) or near wild-type (defecation cycle length) values (Table 3). Note that all transgenes containing *gro-1* appear to slightly slow down the defecation cycle in the wild-type background.

Using pMQ8, we then constructed a *gro-1::gfp* reporter gene (see MATERIALS AND METHODS). This construct (pMQ418) rescues the phenotype to the same degree as pMQ8, indicating that the fusion protein is fully active. The green fluorescent protein (GFP) expression was very mosaic but essentially every cell could be observed to express it in at least a subset of animals (data not shown). The subcellular pattern of expression was diffuse, filling the entire cell (Figure 4, A–D and F). In some cells (most frequently in neurons) the fluorescence in the nucleus was less intense than in the cytoplasm (Figure 4G). This broad subcellular localization is consistent with the findings in yeast, in which the two products of *MOD5* are distributed uniformly in the nucleus, cytoplasm, and mitochondria (GILLMAN *et al.* 1991; TOLERICO *et al.* 1999).

In yeast, the subcellular distribution of Mod5p is achieved by the production of two different proteins from the same transcript by alternative translation initiation (GILLMAN *et al.* 1991). The longer form (Mod5p-I) contains a mitochondrial targeting sequence but some of the protein remains extramitochondrial. The

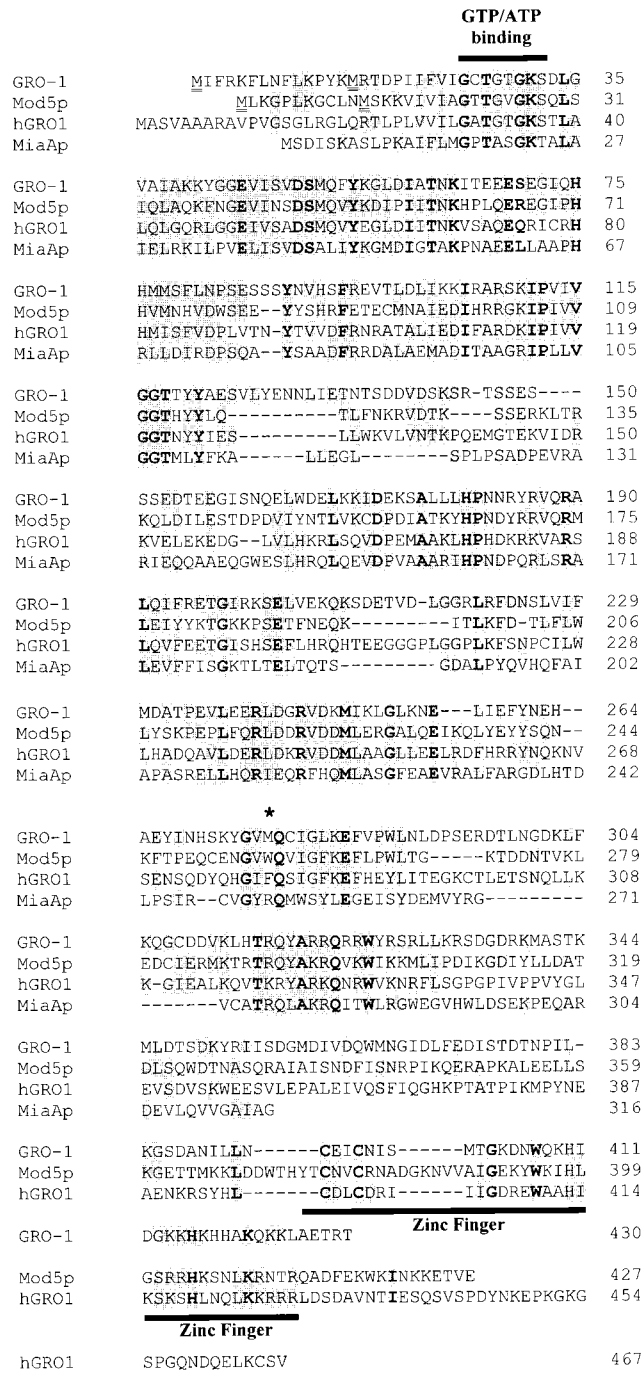

FIGURE 3.—Alignment of GRO-1 with some of its homologs: GRO-1 (*C. elegans*), Mod5p (*S. cerevisiae*), human IPT (hGRO1), and MiaAp (*E. coli*). Conserved amino acids are highlighted in gray, and amino acids conserved in all four sequences are in boldface type. The site of the *e2400* lesion is indicated with an asterisk. *e2400* is a small rearrangement starting at nucleotide 2720 of ZC395 (the sequence TGCAAT GTA is replaced by GC) and resulting in a frameshift. The two alternative initiator methionines are indicated by double underlining in the Mod5p and GRO-1 sequences.

shorter form (Mod5p-II) is produced by initiation from the next ATG in the open reading frame and is partitioned between the cytoplasm and the nucleolus. In Figure 3, the two first methionines of Mod5p and GRO-1 are highlighted by a double underline. To study whether the wide distribution observed with GRO-1::GFP was achieved in a way similar to that of Mod5p, we used site-directed mutagenesis to change the first or the second ATG in the coding sequence (residue 15) to ATC (isoleucine). We also introduced a frameshift between the two ATGs by deleting an A at position 33 of the nucleotide sequence, starting with the A of the first ATG. Thus, two constructs, *gro-1*(Met1Ile)*::gfp* and *gro-1*(DelA33)*::gfp*, should be able to produce only a short form of the protein starting at the second methionine, lacking the mitochondrial localization sequence. Both these constructs gave strong expression and showed a distribution that appeared identical to that of the unmodified *gro-1::gfp* sequence (Figure 4F). However, an absence of fluorescence in the mitochondria could probably not have been observed within a broadly fluorescent cytoplasm. Neither of the two constructs was capable of rescuing the mutant phenotype.

In contrast to the short forms, the *gro-1*(Met15Ile)*::gfp* construct appeared to be expressed exclusively in the mitochondria (Figure 4, E and I) in a pattern indistinguishable from that of other mitochondrial proteins (Figure 4H). This construct was able to rescue the mutant phenotype, including those features that were precisely quantified (Table 3). Taken together, these findings strongly suggest that GRO-1 is normally distributed throughout the cell and that two forms of the protein are produced by the use of alternative translation initiation sites. Furthermore, they indicate that it is the absence of wild-type *gro-1* activity in the mitochondria that is responsible for the phenotypes we observe in the mutant.

DISCUSSION

Maternal rescue of *gro-1* mutants: We show here that *gro-1(e2400)* mutants have a highly pleiotropic phenotype, including altered developmental, behavioral, and reproductive rates. Furthermore, *gro-1(e2400)* increases life span, albeit in a manner that depends in part on the genetic background. The *gro-1* phenotype can be rescued by a maternal effect, so that homozygous *gro-1* mutants produced by a heterozygous mother are virtually indistinguishable from wild-type animals. There are many indications (GOLOVKO *et al.* 2000; STANFORD *et al.* 2000) that the metazoan homologs of MiaAp/Mod5p are also modifying tRNAs. tRNAs, however, are abundant molecules whose total number is likely to increase in parallel with the volume of the animal, which increases >500-fold during postembryonic development. The finding of an almost complete maternal rescue is therefore surprising. GRO-1 would have to be an ex-

TABLE 3

Transgenic expression of GRO-1, GRO-1::GFP, and GRO-1::GFP with altered distribution

Genotype[a]	Defecation cycle length (sec)	Postembryonic development (hr)
gro-1(+)	55.3 ± 3.6 (n = 28)	60.3 ± 0.4 (n = 310)
gro-1(e2400)	93.2 ± 9.2 (n = 28)	104.9 ± 4.7 (n = 126)
gro-1(+);qmEx217[gro-1; (pMQ8)]	65.5 ± 6 (n = 24)	64.7 ± 4.2 (n = 56)
gro-1(e2400);qmEx218[gro-1; (pMQ8)]	69.2 ± 7.4 (n = 28)	68.1 ± 0.1 (n = 53)
gro-1(+);qmEx215[gro-1::gfp; (pMQ418)]	67.7 ± 8.8 (n = 25)	64 ± 2.3 (n = 85)
gro-1(e2400); qmEx219[gro-1::gfp; (pMQ418)]	64.7 ± 7.6 (n = 25)	69.5 ± 6.6 (n = 44)
gro-1(e2400);qmEx211[gro-1::gfp; (pMQ418)]	68.9 ± 6.1 (n = 25)	66.3 ± 4.4 (n = 81)
*gro-1(+);qmEx220[gro-1(*Met1Ile*)::gfp; (pMQ420)]*	66.4 ± 7.0 (n = 21)	61.4 ± 2.7 (n = 87)
*gro-1(e2400);qmEx214[gro-1(*Met1Ile*)::gfp; (pMQ420)]*	84.7 ± 9.5 (n = 19)	97.5 ± 8.9 (n = 59)
*gro-1(+);qmEx221[gro-1(*Met15Ile*)::gfp; (pMQ421)]*	69.9 ± 7.5 (n = 14)	56.1 ± 5.9 (n = 91)
*gro-1(e2400);qmEx216[gro-1(*Met15Ile*)::gfp; (pMQ421)]*	61.0 ± 4.9 (n = 25)	63.8 ± 4.4 (n = 118)
*gro-1(e2400);qmEx213[gro-1(*DelA33*)::gfp; (pMQ419)]*	87.2 ± 16.4 (n = 25)	100.9 ± 9.9 (n = 51)

[a] The names of the clones microinjected to form the extrachromosomal arrays are given in parentheses. The construction of the clones is described in MATERIALS AND METHODS.

tremely stable and active protein (which is not the case in bacteria; LEUNG *et al.* 1997) for the heterozygous mother's contribution of material to the egg (mRNA or protein) to be sufficient to carry out the gene's function adequately in the much larger adult animal. On the basis of similar observations with the *clk-1* gene we suggested an alternate model: that the presence of maternally contributed GRO-1 early during embryonic development could establish an epigenetic state that can last throughout development (WONG *et al.* 1995; BRANICKY *et al.* 2000). Investigations of the levels of the GRO-1 protein, and of modified tRNAs, during the development of maternally rescued animals will help to distinguish between these alternatives.

Subcellular localization of GRO-1: *mod5* encodes IPT in yeast (DIHANICH *et al.* 1987), and its gene product exists in two forms: one form that is found in the mitochondria (where it modifies mitochondrial tRNAs) and in the cytoplasm and one form that is found in the cytoplasm and the nucleus (MARTIN and HOPPER 1982; GILLMAN *et al.* 1991; BOGUTA *et al.* 1994; TOLERICO *et al.* 1999). These two forms differ by only a short N-terminal sequence whose presence or absence is determined by differential translation initiation at two "in frame" ATG codons (GILLMAN *et al.* 1991). The *gro-1* open reading frame also contains two ATG codons at comparable positions, with the coding sequence between the two codons constituting a plausible mitochondrial sorting signal. We found that a GRO-1::GFP fusion protein is localized throughout the cell. When the first putative initiator ATG is removed by site-directed mutagenesis, GRO-1 is still abundantly expressed in the cytoplasm and nucleus, indicating that the second ATG is a good initiator codon. Furthermore, when the second initiator ATG of *gro-1* is removed, GRO-1 is localized exclusively to the mitochondria. These findings strongly suggest that the cellular distribution of GRO-1 is achieved by mechanisms very similar to those observed in yeast with Mod5p.

MiaAp, the bacterial homolog of GRO-1, regulates gene expression: Mutations in *miaA,* the bacterial homolog of *gro-1,* have broadly pleiotropic consequences in various bacteria species, including effects on growth rate (DIAZ *et al.* 1987), on the rate of spontaneous GC → TA transversions (CONNOLLY and WINKLER 1989) in *E. coli*, on the regulation of the biosynthesis of amino acids in *Salmonella typhimurium* (ERICSON and BJORK 1986; BLUM 1988), and on the regulation of virulence genes in *Shigella flexneri* (GRAY *et al.* 1992). In Shigella, it was found that the level of the virulence-associated protein

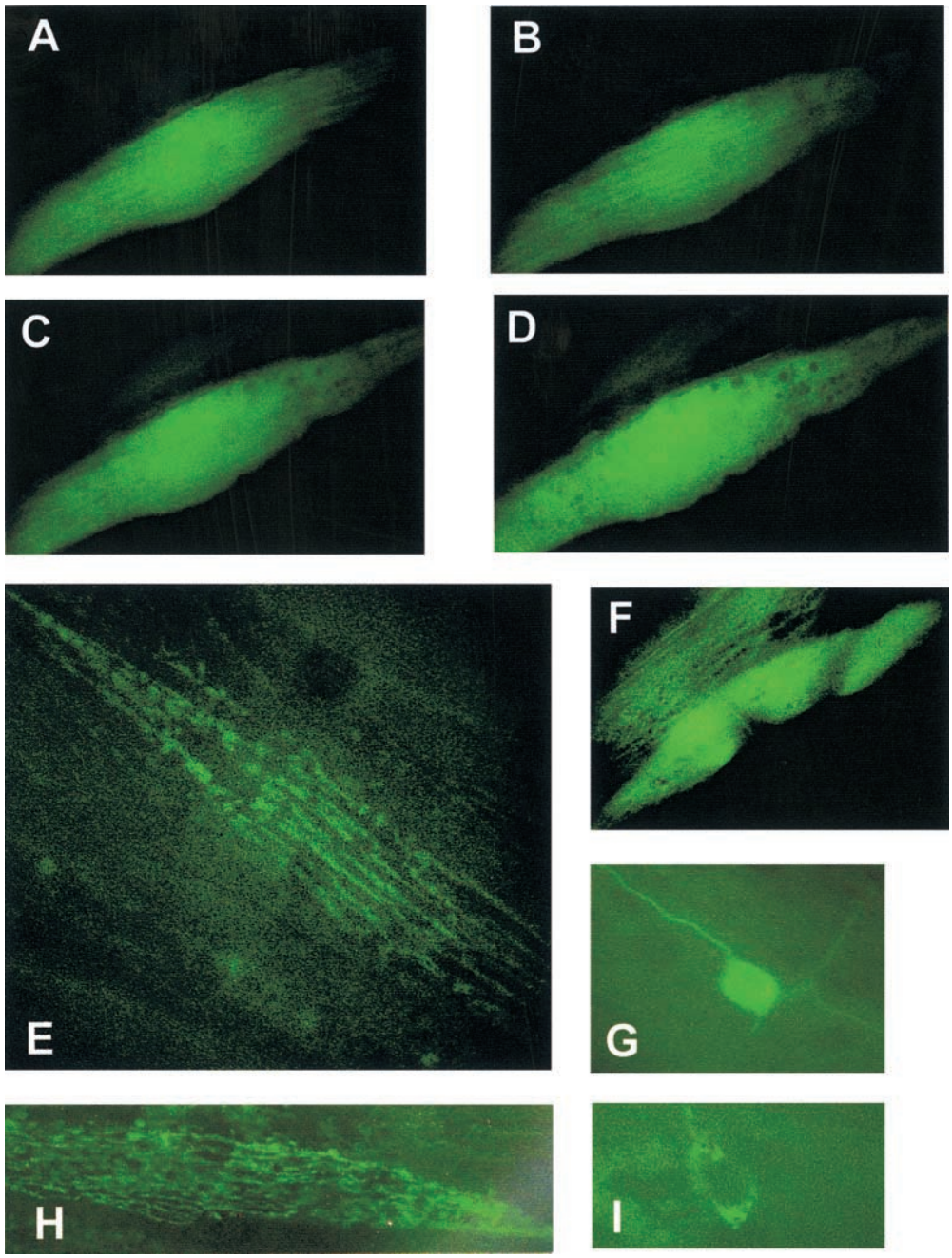

FIGURE 4.—Subcellular expression of GRO-1::GFP. (A–D) GFP fluorescence in a muscle cell in three different planes of focus to show how the fluorescence pervades the entire cytoplasm and nucleus. The weak striations that can be observed are the results of partial exclusion of the fluorescence from the contractile elements of the muscle. The dark granules that can be seen in D are not mitochondria but some other unidentified cytoplasmic inclusions. (E) Mitochondrial localization of the long form of GRO-1 [product of *gro-1(*Met1-5Ile*)::gfp*; see main text]. The mitochondrial distribution of CLK-1 is shown in H for comparison. (F) A muscle cell adjacent to the vulva expressing the short form of GRO-1 [product of *gro-1(*Met1Ile*)::gfp*; see main text]. Only one plane of focus is shown. The observed distribution is indistinguishable from the distribution of GRO-1::GFP as shown in A–D. (G) Distribution of GRO-1::GFP in a neuron. Note the fluorescence is also found in the neuronal projection and that it is slightly less intense in the nucleus. (H) The mitochondrial distribution of CLK-1 (FELKAI *et al.* 1999). (I) Distribution of the long form of GRO-1 in the mitochondria of a neuron. Note the granular cytoplasmic distribution and the exclusion from the nucleus.

VirF was reduced 10-fold in the mutant but that the level of mRNA was unaffected. These observations together with the fact that MiaAp modifies a component of the translation machinery suggested that *miaA* acts by post-transcriptional mechanisms (BJORK *et al.* 1999).

The function of GRO-1 in mitochondria: We found that it is the mitochondrially expressed form of GRO-1 that is important for the dramatic phenotypes we observe in the mutant. Our findings thus suggest that a broad regulatory function for IPT has been conserved from bacteria to the mitochondria of metazoans. As in most animals, the number of proteins encoded and expressed in the mitochondria of nematodes is fairly limited (KEDDIE *et al.* 1998), and all of them are elements of the respiratory chain. However, the respiration, ATP levels, and metabolic capacity of *gro-1* mutants do not appear to be strongly affected (BRAECKMAN *et al.* 1999). If GRO-1 exercises its effect by acting on translation only, the actual translation defect in the mutant must be relatively subtle as it does not grossly impair mitochondrial function. Thus, at present it is unclear what defect produces the major phenotypic effects we observe in the mutants.

As described in the Introduction, *clk-1* is another gene that affects physiological rates and can produce a maternal effect (WONG *et al.* 1995). As CLK-1 is a mitochondrial protein (FELKAI *et al.* 1999), to explain all the phenotypic features of *clk-1* mutants, in particular the mito-

chondrial localization, the maternal effect, and the absence of major metabolic defects, we hypothesized that CLK-1 affects, perhaps indirectly, the cross talk between the mitochondria and the nucleus (Branicky *et al.* 2000). Such cross talk would be useful in allowing the pattern of nuclear gene expression to be modulated in response to the metabolic state of the cell. In this model, during early development the presence of CLK-1 or GRO-1 in the mitochondria of maternally rescued *clk-1* or *gro-1* mutants, respectively, would allow the presence of metabolically competent mitochondria to be signaled to the nucleus. This in turn could lead to the establishment of a stable pattern of gene expression resulting in a wild-type phenotype, that is, rapid growth, behavior, and reproduction throughout the life of the animal.

We are grateful to Alan Coulson and Andy Fire for the gift of clones and to Anne Wong for technical assistance. We are particularly grateful to Robyn Branicky for reviewing the manuscript. Some strains used in this work were provided by the Caenorhabditis Genetics Center, which is funded by the National Center for Research Resources of the U.S. National Institutes of Health. This work was supported by a studentship from the Medical Research Council (MRC) of Canada to J.L., by a studentship from the Fonds pour la Formation de Chercheurs et l'Aide à la Recherche to B.L., and by grants from the MRC of Canada to S.H.

LITERATURE CITED

Amuthan, G., G. Biswas, S. Y. Zhang, A. Klein-Szanto, C. Vijayasarathy *et al.*, 2001 Mitochondria-to-nucleus stress signaling induces phenotypic changes, tumor progression and cell invasion. EMBO J. **20:** 1910–1920.

Bartz, J. K., L. K. Kline and D. Soll, 1970 N6-(Delta 2-isopentenyl)adenosine: biosynthesis in vitro in transfer RNA by an enzyme purified from Escherichia coli. Biochem. Biophys. Res. Commun. **40:** 1481–1487.

Biswas, G., O. A. Adebanjo, B. D. Freedman, H. K. Anandatheerthavarada, C. Vijayasarathy *et al.*, 1999 Retrograde Ca2+ signaling in C2C12 skeletal myocytes in response to mitochondrial genetic and metabolic stress: a novel mode of inter-organelle crosstalk. EMBO J. **18:** 522–533.

Bjork, G. R., J. M. Durand, T. G. Hagervall, R. Leipuviene, H. K. Lundgren *et al.*, 1999 Transfer RNA modification: influence on translational frameshifting and metabolism. FEBS Lett. **452:** 47–51.

Blum, P. H., 1988 Reduced leu operon expression in a miaA mutant of Salmonella typhimurium. J. Bacteriol. **170:** 5125–5133.

Boguta, M., L. A. Hunter, W. C. Shen, E. C. Gillman, N. C. Martin *et al.*, 1994 Subcellular locations of MOD5 proteins: mapping of sequences sufficient for targeting to mitochondria and demonstration that mitochondrial and nuclear isoforms commingle in the cytosol. Mol. Cell. Biol. **14:** 2298–2306.

Braeckman, B. P., K. Houthoofd, A. De Vreese and J. R. Vanfleteren, 1999 Apparent uncoupling of energy production and consumption in long-lived Clk mutants of Caenorhabditis elegans. Curr. Biol. **9:** 493–496.

Branicky, R., C. Benard and S. Hekimi, 2000 clk-1, mitochondria, and physiological rates. Bioessays **22:** 48–56.

Caillet, J., and L. Droogmans, 1988 Molecular cloning of the Escherichia coli miaA gene involved in the formation of delta 2-isopentenyl adenosine in tRNA. J. Bacteriol. **170:** 4147–4152.

Connolly, D. M., and M. E. Winkler, 1989 Genetic and physiological relationships among the miaA gene, 2-methylthio-N6-(delta 2-isopentenyl)-adenosine tRNA modification, and spontaneous mutagenesis in Escherichia coli K-12. J. Bacteriol. **171:** 3233–3246.

Diaz, I., S. Pedersen and C. G. Kurland, 1987 Effects of miaA on translation and growth rates. Mol. Gen. Genet. **208:** 373–376.

Dihanich, M. E., D. Najarian, R. Clark, E. C. Gillman, N. C. Martin *et al.*, 1987 Isolation and characterization of MOD5, a gene required for isopentenylation of cytoplasmic and mitochondrial tRNAs of Saccharomyces cerevisiae. Mol. Cell. Biol. **7:** 177–184.

Ericson, J. U., and G. R. Bjork, 1986 Pleiotropic effects induced by modification deficiency next to the anticodon of tRNA from Salmonella typhimurium LT2. J. Bacteriol. **166:** 1013–1021.

Ewbank, J. J., T. M. Barnes, B. Lakowski, M. Lussier, H. Bussey *et al.*, 1997 Structural and functional conservation of the Caenorhabditis elegans timing gene clk-1. Science **275:** 980–983.

Felkai, S., J. J. Ewbank, J. Lemieux, J. C. Labbe, G. G. Brown *et al.*, 1999 CLK-1 controls respiration, behavior and aging in the nematode Caenorhabditis elegans. EMBO J. **18:** 1783–1792.

Frohman, M. A., M. K. Dush and G. R. Martin, 1988 Rapid production of full-length cDNAs from rare transcripts: amplification using a single gene-specific oligonucleotide primer. Proc. Natl. Acad. Sci. USA **85:** 8998–9002.

Frolov, M. V., E. V. Benevolenskaya and J. A. Birchler, 2000 The oxen gene of Drosophila encodes a homolog of subunit 9 of yeast ubiquinol-cytochrome c oxidoreductase complex: evidence for modulation of gene expression in response to mitochondrial activity. Genetics **156:** 1727–1736.

Gillman, E. C., L. B. Slusher, N. C. Martin and A. K. Hopper, 1991 MOD5 translation initiation sites determine N6-isopentenyladenosine modification of mitochondrial and cytoplasmic tRNA. Mol. Cell. Biol. **11:** 2382–2390.

Golovko, A., G. Hjalm, F. Sitbon and B. Nicander, 2000 Cloning of a human tRNA isopentenyl transferase. Gene **258:** 85–93.

Gray, J., J. Wang and S. B. Gelvin, 1992 Mutation of the miaA gene of Agrobacterium tumefaciens results in reduced vir gene expression. J. Bacteriol. **174:** 1086–1098.

Hekimi, S., 2000 Crossroads of aging in the nematode Caenorhabditis elegans. Results Probl. Cell Differ. **29:** 81–112.

Hekimi, S., P. Boutis and B. Lakowski, 1995 Viable maternal-effect mutations that affect the development of the nematode *Caenorhabditis elegans*. Genetics **141:** 1351–1364.

Hekimi, S., B. Lakowski, T. M. Barnes and J. J. Ewbank, 1998 Molecular genetics of life span in C. elegans: how much does it teach us? Trends Genet. **14:** 14–20.

Hodgkin, J., and T. Doniach, 1997 Natural variation and copulatory plug formation in *Caenorhabditis elegans*. Genetics **146:** 149–164.

Huang, X. Y., and D. Hirsh, 1989 A second trans-spliced RNA leader sequence in the nematode Caenorhabditis elegans. Proc. Natl. Acad. Sci. USA **86:** 8640–8644.

Hwang, K. Y., J. H. Chung, S. H. Kim, Y. S. Han and Y. Cho, 1999 Structure-based identification of a novel NTPase from Methanococcus jannaschii. Nat. Struct. Biol. **6:** 691–696.

Jonassen, T., P. L. Larsen and C. F. Clarke, 2001 A dietary source of coenzyme Q is essential for growth of long-lived Caenorhabditis elegans clk-1 mutants. Proc. Natl. Acad. Sci. USA **98:** 421–426.

Keddie, E. M., T. Higazi and T. R. Unnasch, 1998 The mitochondrial genome of Onchocerca volvulus: sequence, structure and phylogenetic analysis. Mol. Biochem. Parasitol. **95:** 111–127.

Kenyon, C., J. Chang, E. Gensch, A. Rudner and R. Tabtiang, 1993 A C. elegans mutant that lives twice as long as wild type. Nature **366:** 461–464.

Lakowski, B., and S. Hekimi, 1996 Determination of life-span in Caenorhabditis elegans by four clock genes. Science **272:** 1010–1013.

Leung, H. C., Y. Chen and M. E. Winkler, 1997 Regulation of substrate recognition by the MiaA tRNA prenyltransferase modification enzyme of Escherichia coli K-12. J. Biol. Chem. **272:** 13073–13083.

Martin, N. C., and A. K. Hopper, 1982 Isopentenylation of both cytoplasmic and mitochondrial tRNA is affected by a single nuclear mutation. J. Biol. Chem. **257:** 10562–10565.

Miyadera, H., H. Amino, A. Hiraishi, H. Taka, K. Murayama *et al.*, 2001 Altered quinone biosynthesis in the long-lived clk-1 mutants of Caenorhabditis elegans. J. Biol. Chem. **276:** 7713–7716.

Noskov, V. N., K. Staak, P. V. Shcherbakova, S. G. Kozmin, K. Negishi *et al.*, 1996 HAM1, the gene controlling 6-N-hydroxylaminopurine sensitivity and mutagenesis in the yeast Saccharomyces cerevisiae. Yeast **12:** 17–29.

Sekito, T., J. Thornton and R. A. Butow, 2000 Mitochondria-to-nuclear signaling is regulated by the subcellular localization of the transcription factors Rtg1p and Rtg3p. Mol. Biol. Cell **11:** 2103–2115.

Stanford, D. R., N. C. Martin and A. K. Hopper, 2000 ADEPTs: information necessary for subcellular distribution of eukaryotic sorting isozymes resides in domains missing from eubacterial and archaeal counterparts. Nucleic Acids Res. **28:** 383–392.

Tolerico, L. H., A. L. Benko, J. P. Aris, D. R. Stanford, N. C. Martin *et al.*, 1999 *Saccharomyces cerevisiae* Mod5p-II contains sequences antagonistic for nuclear and cytosolic locations. Genetics **151:** 57–75.

Wong, A., P. Boutis and S. Hekimi, 1995 Mutations in the clk-1 gene of *Caenorhabditis elegans* affect developmental and behavioral timing. Genetics **139:** 1247–1259.

Zorio, D. A., N. N. Cheng, T. Blumenthal and J. Spieth, 1994 Operons as a common form of chromosomal organization in C. elegans. Nature **372:** 270–272.

Communicating editor: P. Anderson